Vibrational Entropy Driven Unusual Phase Transition in A Hybrid Organic-Inorganic Perovskite

Wenjuan Wei[1], Wei Li[1*], Keith T. Butler[2*], Guoqiang Feng[1], Christopher J. Howard[3], Song Gao[4*], Michael A. Carpenter[5*], Peixiang Lu[1] and Aron Walsh[6]

[1]*Department of Physics, Huazhong University of Science & Technology, Luoyu Road, Wuhan, China*

[2]*Department of Chemistry, University of Bath, Claverton Down, Bath BA2 7AY, UK*

[3]*School of Engineering, University of Newcastle, New South Wales 2308, Australia*

[4]*College of Chemistry and Molecular Engineering, Peking University, Beijing 100871, China*

[5]*Department of Earth Sciences, University of Cambridge, Downing Street, Cambridge, CB2 3EQ, UK*

[6]*Department of Materials, Imperial College London, Royal School of Mines, Exhibition Road, London SW7 2AZ, UK*

Phase transitions (PTs) of ABX_3 hybrid organic-inorganic perovskites (HOIPs) can endow many important electrical, magnetic and optical properties which are the key for their applicable functionalities. In this context, elucidating their mechanisms has become an essential forefront in the field. Hitherto, the driving forces of their PTs are limited to the BX_6 octahedral tilting and molecular ordering of the A-site, while other atomic factors have attracted little attention. Herein, we uncover a complex ferroelastic PT in a HOIP, $[CH_3NH_3][Mn(N_3)_3]$, based on thermodynamic experiments and *ab initio* lattice dynamics calculations. This unusual first-order PT, between two ordered phases, is primarily driven by collective atomic vibrations of the whole lattice, along with concurrent molecular displacement and peculiar octahedral tilting. Moreover, the unique atomic vibrational gain is the origin of the significant entropy change between the low and high temperature structures, and in return it plays a critical role in driving the transition. This finding offers an alternative pathway for designing new ferroic PTs and related physical properties in HOIPs and other hybrid crystals.

*e-mail: wl276@hust.edu.cn; k.t.bulter@bath.ac.uk

gaosong@pku.edu.cn; mc43@esc.cam.ac.uk

Hybrid organic-inorganic perovskites (HOIPs) have attracted growing interest in the past several years due to their superior application potentials in the field of photovoltaics, optoelectronics and sensing devices[1]. Similar to their conventional oxide counterparts, these HOIPs exhibit abundant structural transitions in response to external perturbations such as temperature or pressure[2,3]. Since these phase transitions can often endow significant changes in the electrical, magnetic and optical properties which are of vital importance for the design and fabrication of functional devices, it is crucial to fully understand their origins from an atomic scale. For example, it has been found that the first-order tetragonal-to-orthorhombic transition of $MAPbI_3$ below 160 K, driven by the soft modes of PbI_6 octahedral tilting and the MA cation ordering, could have a significant impact on its electron-phonon coupling and corresponding photovoltaic properties[4].

In traditional inorganic perovskites, the A-site displacement and BX_6 octahedral tilting are the primary driving forces of phase transitions, however, the presence of organic species on the A- and/or X-sites in HOIPs significantly complicate the symmetry breaking process[2,5]. Though octahedral tilting patterns in HOIPs are generally reminiscent of those in conventional perovskites due to the rigidity of the X-site molecular linkers, these much larger and longer X-sites offer additional freedom for the octahedra to tilt, hence offering new tilting pathways. The recent discovery that adjacent octahedra in [TMA][$Mn(N_3)_3$] (TMA = tetramethylammonium) distort along the same direction indeed proves such new possibilities[6]. On the other hand, the dynamic movement of the organic A-site from one state to another, which normally appears as order-disorder switching via rotational and configurational changes, can also induce symmetry changes[7]. It is worth of mentioning that accompanying alterations of hydrogen bonding and dispersive forces during the dynamic switching will in turn influence the phase transition. Such complex synergies in the A-site have been found to

be the main origin of ferroelectricity in some HOIPs (i.e. [DMA][$Co(HCOO)_3$], DMA = dimethylammonium)[8], in stark contrast to the displacive nature of electrical ordering in perovskite oxides (e.g. $BaTiO_3$)[9].

Although the importance of phase transitions of HOIPs has attracted increasing awareness, most studies were focused on the aforementioned driving factors of molecular displacement and ordering[2]. As one prominent difference between HOIPs and inorganic perovskites is their atomic weight, the presence of substantially lighter elements such as hydrogen and carbon could lead to remarkable energetic changes across the transition if their vibrational entropic effects are large enough. Such vibrational entropy effects have been found to be the important factor for driving the polymorphism in hybrid formates by recent lattice dynamics calculations[10]. Herein, we report the very unusual vibrational entropy driven phase transition in an azide HOIP, [MA][$Mn(N_3)_3$] on the basis of comprehensive structural and thermodynamic characterisations, as well as extensive lattice dynamics calculations. We unveil that the complex first-order phase transition in [MA][$Mn(N_3)_3$] is akin to the synergistic motions of the octahedral tilting, rotation and displacement of the MA cation, motion of the azide group and the vibration of all atoms. We also demonstrate that the significant entropy change across the transition arises from the vibrational effects of all atoms which in return are the major source for thermally driving the phase transition.

1 has an ABX_3 perovskite structure, in which the *A*-, *B*- and *X*-sites are MA, Mn^{2+} and azide group, respectively. The HT structure in $P2_1/c$ is on a cell (1,1,0), (-1,1,0), (0,0,2) with an origin of (0,1/2,1/2) with respect to a perovskite parent, which could be from a combination of the irrep M_3^- and conventional out-of-phase tilt, R_4^+. Therefore, the transition, from the cubic parent to HT phase, would be from the conventional system R_4^+ at k =

1/2,1/2,1/2 to tilt system Σ_2 at k = 1/4,1/4,0 in the Brillouin zone, from the group theory program ISOTROPY[13]. The LT $P2_1/c$ structure proposed here is on a cell (0,1,0), (-1,0,1), (2,0,2) with an origin (0,0,1/2) with respect to a perovskite parent. The irreducible representation (irrep) Σ_2 at k = 1/4,1/4,0 is critical in this structure as this is the only irrep that would give the very unusual pattern of tilts[13]. Originally, we would obtain an orthorhombic *Pbam* structure since the out-of-phase tiltings run alternatively clockwise and anticlockwise in the *ab* plane, reminiscent of the tilt senses in a standard perovskite. This irrep that will induce these displacements is M_3^-. However, the zig-zag (up-down) tilting patterns, when viewing the octahedra side-on along *b* or *c*-axis, is significantly unusual. This distortion may be driven by the locations of the cavity MA entities because Σ_2 at k = 1/4,1/4,0 and M_3^- at k=1/2,1/2,0 in the Brillouin zone would give the required $P2_1/c$ space group[5].

The high temperature (HT) structure (270 K, Figure 1a) of **1** crystalizes in the monoclinic space group $P2_1/c$, with a = 9.0316(10), b = 7.3935(8), c = 12.5458(13) Å, β = 102.429(11)° and V = 818.12(15) Å^3, in which the fully ordered MA^+ is hydrogen-bonded to the $[Mn(N_3)_3]^-$ perovskite framework[11]. There are four hydrogen bonds in each pseudo-perovskite unit and the N···N distances and N-H···N angles are of 2.966(3)-3.127(3) Å and 146.9(4)-170.5(4)°, respectively. Notably, the MA cation is located in the perovskite cavity at an off-center position along the *c*-axis and the adjacent MnN_6 octahedra distort along this direction. According to the Glazer notation, the octahedral tilting system of the HT phase would be $a^+b^+c^-$[12]. Like conventional perovskites, this HT structure could have a parent cubic structure with space group *Pm*-3*m* and cell parameter a_c, and the cell dimensions of this $P2_1/c$ structure are $\sqrt{2}a_c$* $\sqrt{2}a_c$* $2a_c$.

Upon cooling, compound **1** undergoes a phase transition at about 264 K, and the low temperature (LT) phase crystalizes in the same monoclinic space group $P2_1/c$ with a = 6.2218(4), b = 7.2500(4), c = 18.3398(11) Å, β = 102.075(5)° and V = 808.97(8) Å^3 (Figure 1b)[11]. Interestingly, the a_{LT} and c_{LT} axes are about half of c_{HT} and twice of a_{HT}, respectively, while the *b*-axis is almost unchanged. This fact indicates that the perovskite structure undergoes a significant re-construction across the transition. This transition has a complex cooperative nature which involves all the *A*-, *B*- and *X*-sites. Specifically, the MA cation exhibits both displacement and rotation about the C-N axis, and the MnN_6 octahedra tilt dramatically along with the significant movement of the azide groups. Such a synergistic transformation leads to the breaking and reforming of hydrogen bonding with N···N distances of 2.925(2)-3.252(3) Å and N-H···N angles of 149.2(3)-158.6(3)° (Figure 1b). Strikingly, three newly constructed hydrogen bonds in this LT phase are about 1.3-4.0% longer than those in the HT structure though the fourth one is slightly shorter (1.4%) (Figure 1c). This results in the overall weakening of the hydrogen-bonding when crossing the transition from HT to LT phase, which has not occurred in any other HOIPs[2]. However, the thermal vibrations of all atoms in **1** show a normal trend, where the atomic displacement parameters (ADPs) of C, N_A, Mn and N_X all decrease upon cooling (Figure 1d). Additional solid state ^{1}H magic-angle spinning nuclear magnetic resonance (MAS NMR) measurements reveal the thermal vibration of hydrogen atoms in the perovskite structure. As seen from Figure S3a, the chemical shift of hydrogen atoms on the $–NH_3$ group reduces from 6.6 to 6.3 ppm with decreasing intensity when cooling from 323 to 223 K, which indicates increasing shielding effects of the nitrogen atom with respect to the attached hydrogens, hence weakening the vibration of amino hydrogens upon cooling. Such an unusual phenomenon arises from the competing effects between the electrostatic interactions and hydrogen bonding in the perovskite unit across the transition. The unit cell volume contracts about 0.35%

when cooling from 270 to 260 K, this significant volume change leads to an increase of electrostatic interactions between the MA cation and the perovskite host, which compensates the lengthening of the hydrogen bonding and result in decreasing ADPs from HT to LT. Another interesting feature of the transition is that the azide group exhibits both *cis*-EE and *trans*-EE coordination modes rather than pure *cis*-EE fashion in the HT phase[11]. The Glazer notation for octahedral tilting of this LT structure is not applicable, and the cell dimensions of this LT structure are a_c* $\sqrt{2}a_c$* $2\sqrt{2}a_c$ of the parent cubic *Pm*-3*m* structure.

DSC experiments provide thermodynamic information about the transition (Figure S2a). The temperature dependencies of heat flows show an anomaly at 277 K on heating and at 264 K on cooling, in agreement with the literature[11]. The width of the thermal hysteresis of 13 K and sharp peaks observed at both heating and cooling indicate the strong first-order nature of the phase transition. Temperature dependencies of entropy (S), shown in Figure S2b, demonstrate that the associated entropy change (ΔS) across the phase transition is approximately 20 J $K^{-1}kg^{-1}$. Such a significant value is close to that of a two-fold order-disorder transition ($\Delta S = R\ln N_2/N_1 = R\ln 2 = 27$ J $K^{-1}kg^{-1}$, where N represents the ratio of possible configurations after and before phase transition and R is gas constant), though our single crystal X-ray diffraction studies unambiguously exclude the existence of any structural disorder in the HT phase. This unusual phenomenon suggests that the HT lattice exhibits a dramatic increase in the vibrational degrees of freedom and corresponding active phonon modes.

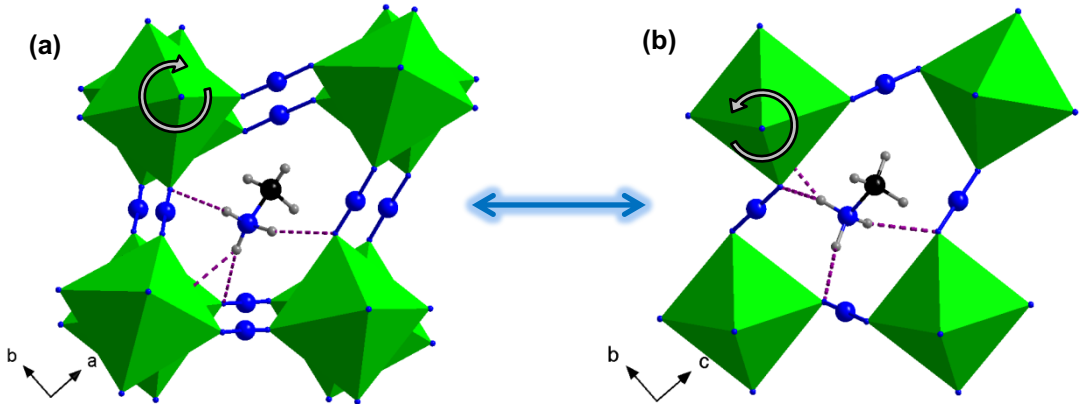

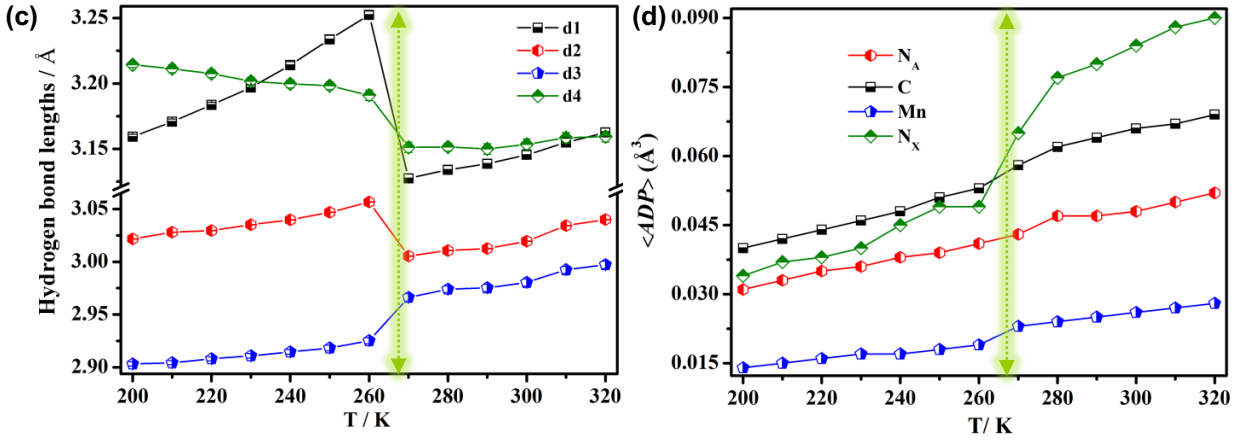

Figure 1. (a) The crystal structure of HT (270 K) viewed from *c* axis. (b) The crystal structure of LT (260 K) viewed from *a* axis. Violet dotted lines signify the hydrogen bonds. The arrows filled with grey point the rotation directions of octahedral during phase transition. Color scheme: Mn^{2+} and MnN_6 octahedron, emerald; C, black; N, blue; H, 25% grey. (c) Hydrogen bond lengths as a function of temperature between 200 to 320 K. (d) Temperature dependencies of atomic displacement parameters of Mn, C, N_A and N_X atoms. Emerald dash lines separate the LT and HT phase regions.

Resonant ultrasound spectroscopy (RUS) experiments were used to probe the thermodynamics of the phase transition. Selected RUS spectra from a single crystal collected during both heating and cooling sequences between 100 to 280 K are shown in Figure S4a. Temperature dependent peaks in the spectra indicate the vibrational frequencies (f) of the sample modes, and the f^2 and the reciprocal of mechanical quality factor (Q^{-1}) of each vibrational mode quantifies the elastic modulus and the acoustic dissipation (energy loss) associated to this mode, respectively[14]. The raw spectra in Figure S4a exhibit an obvious anomaly in terms of peak frequencies near 264 K upon cooling, along with the changes of peak widths and disappearance of some peaks. Data for f^2 obtained from fitting selected cooling peaks, displayed in Figure 2a, demonstrate obvious stiffening kinks at about 264 K, corresponding to the known strong first-order transition. Meanwhile, the acoustic dissipations (Q^{-1}) for all selected frequency peaks increase significantly below 264 K as shown in Figure 2b. The increased frequency can be attributed to the twin walls formed after the ferroelastic

structural reconstruction, which couple with the strain and are mobile in response to the external stress[15]. Strikingly, the energy loss patterns of **1** span near or over a hundred Kelvin, which is a substantially broader range than that associated with a phase transition driven by the configurational order-disorder of the A-site organic amine cations, in $[(CH_2)_3NH_2^+][Mn(HCOO)_3]$[16] and $[(CH_3)_2NH_2^+][Co(HCOO)_3]$[17].

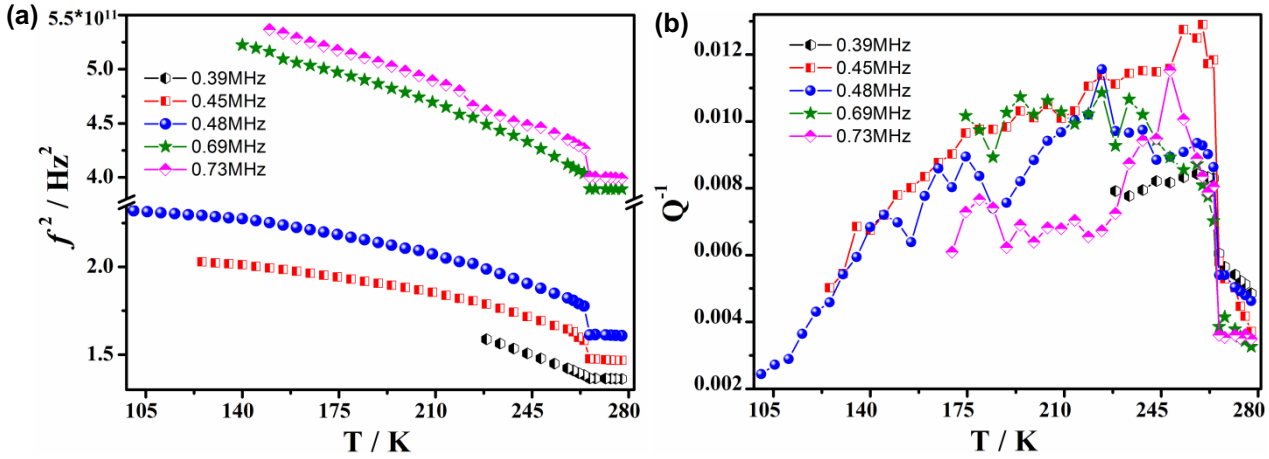

Figure 2. Variation of the f^2 (a) and Q^{-1} (b) from fitting of selected cooling resonance peaks in RUS.

To fully understand the origin of the associated large ΔS and Q^{-1}, we have applied lattice dynamics calculations to probe the atomistic details of the forces driving this phase transition[18-19]. Figure S5a plots the free energy of the two phases versus temperature and the vibrational entropy contribution to the free energy (ΔG) of each phase versus temperature. This plot shows that the vibrational entropy (S_V) of the HT phase is greater than that of the LT phase. As the temperature increases so the S_V contribution to total free energy becomes more pronounced and eventually the HT phase becomes thermodynamically more favourable than the LT phase at a temperature of 220 K. We investigate which phonon modes are responsible for the differences in S_V between the two phases. The contributions of the phonon modes to S_V of two phases are shown in Figure S5b, which displays the most notably contribution at the low-frequency end of the spectrum. The frequency dependencies of S_V and integrated vibrational entropy (S_{Tot}) between HT and LT are plotted in Figures 3a, b. These

figures show how the vibrational modes contribute to the entropy, depending on their frequency. The vast majority of the contribution comes from vibrational modes with frequency below 10 THz. The dashed lines show the total accumulated entropy from the modes up to that frequency - these plateau around 10 THz too. These values are plotted across a range of temperatures.

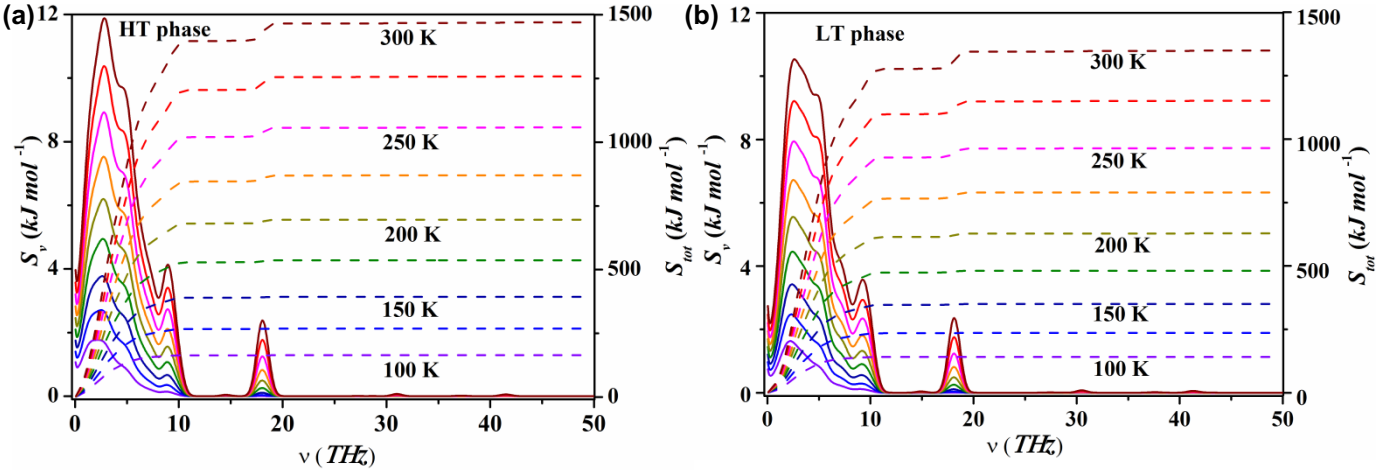

Figure 3. The frequency dependencies of vibrational entropy S_v and integrated vibrational entropy S_{tot} between HT (a) and LT phase (b).

To probe the atomistic origins of the above results, we have decomposed the fractional contribution of each structural site (*A*-, *B*- and *X*-sites) to the S_{Tot} within the corresponding entropy range by calculating the weighted average of the phonon density of states (DOS) of a given site *i* at energy ε, $\langle g_i(\varepsilon)\rangle = \sum_i \omega_i / \sum_{i.k} \omega_{ik}$, where ω_i are the weights of the phonon modes involving the site at energy ε and *k* is the list of all sites[10]. The frequency dependencies of decomposed DOS of each atom at HT and LT are plotted in Figures 4c, d. This shows the contributions to the phonon spectrum broken down by atomic site. As seen from this, the modes that contribute most to the entropy (those at < 10 THz) involve contributions from all species. This shows that these phonons are collective modes, where all of the sites are moving together - these depend on the interactions between the units in the crystal. The collective motions determine the entropy and the collective motions in turn depend on the

strength of the bonding between molecule and the perovskite framework. This is where all of the difference in S_V comes from.

The importance of collective modes in determining thermodynamic stability distinguishes with the trend in other HOIPs (i.e. $[MA][PbI_3]$[20] and $[(CH_2)_3NH_2][Mn(HCOO)_3]$[21]), where dynamic configurational ordering is mainly responsible for the difference in S_V between competing phases. The phase transition is more similar to the ABX_3-type formate, $[NH_4][Zn(HCOO)_3]$[18], which display an entropy-driven polymorphism. However, in this case the balance of forces in this case is different, because in those formates the HT phase features weaker molecule-cavity intermolecular hydrogen bonds than the LT structure, but the molecule-cavity hydrogen bonds in **1** are stronger in the HT phase and the LT phase is more enthalpicaly stable due to the increased electrostatic interactions induced by the lattice contraction.

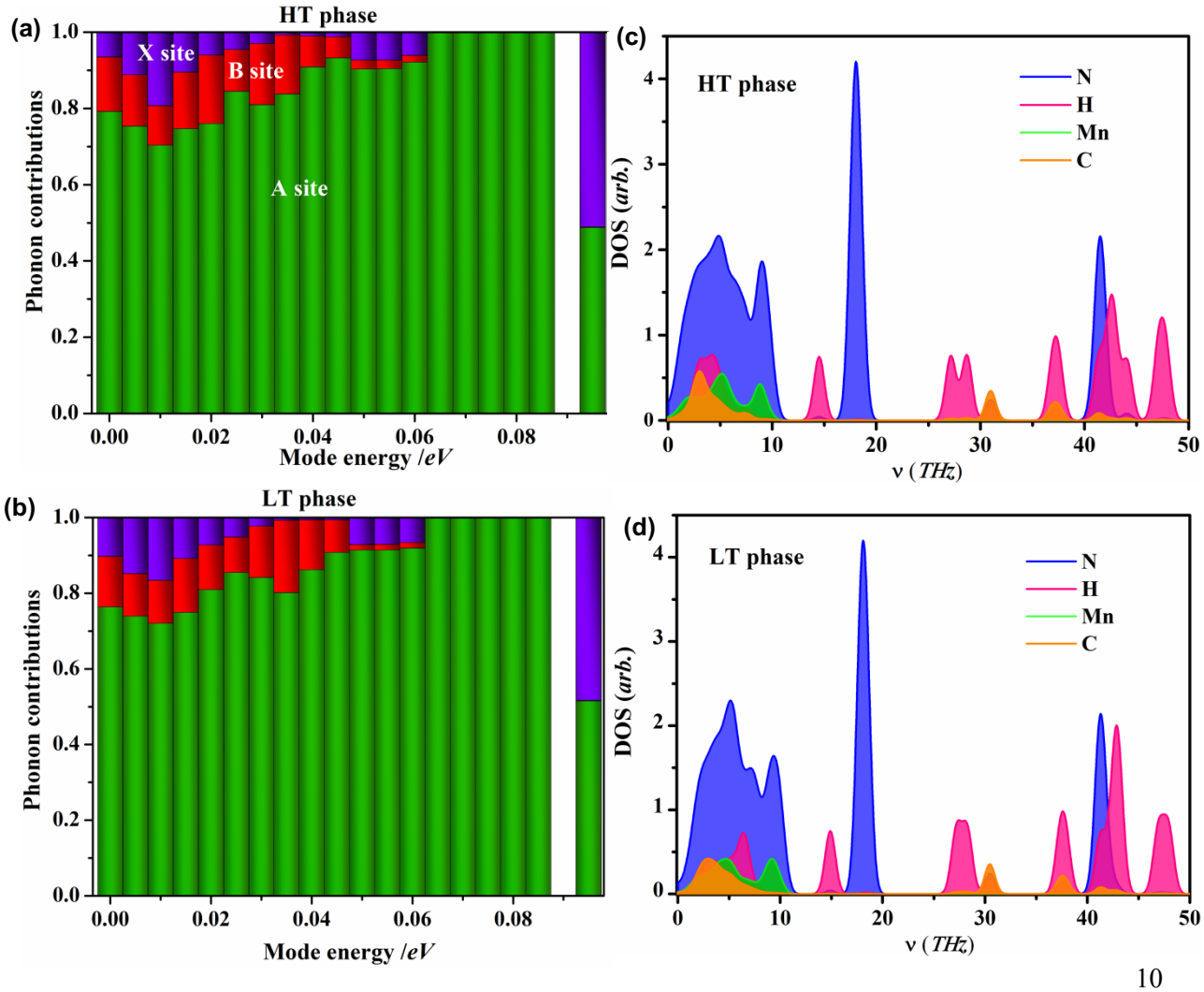

Figure 4. The fractional contribution of *A*-site (green), *B*-site (red) and *X*-site (purple) to the total vibrational entropy at HT (top) (a) and LT (bottom) (b) phase within the 0-0.10 eV energy range. The frequency dependencies of decomposed DOS of each atom at HT (c) and LT phase (d).

Based on the aforementioned extensive calculations, we can now explain the origin of the large entropy change and energy loss across the phase transition. First of all, the synergistic motions of the whole structure, which involve the MnN_6 octahedral tilting, the rotation and displacement of the MA cation, motion of the azide group and the vibration of all atoms, are responsible for the occurrence of the phase transition. In particular, the dominant vibrational entropic effects are the main cause of the structural transition instead of any significant enthalpic or configurational entropy origin. In addition, the collective vibrations of the whole structure also lead to the substantial damping of the structure in response to external stress during the RUS experiments, hence giving rise to significant acoustic dissipation. Nevertheless, extrinsic origins of the energy loss from twinning also need to be taken into account. The mobility of the twin walls during transition is a common inducement to energy loss like observed in other HOIPs[16-17] and perovskite oxides[15]. It is noteworthy that the HT structure at room temperature is already strongly twinned as seen from our optical microscopy measurements (Figures 5a, b). Clearly, there are both parallel (~12.8°) and orthogonal (~83.7 and 82.0°) twin walls. In this context, the effective modulus of the material is reduced by mobile domain boundaries and the friction of twin walls increases the damping of the mechanical resonance during the RUS testing[22].

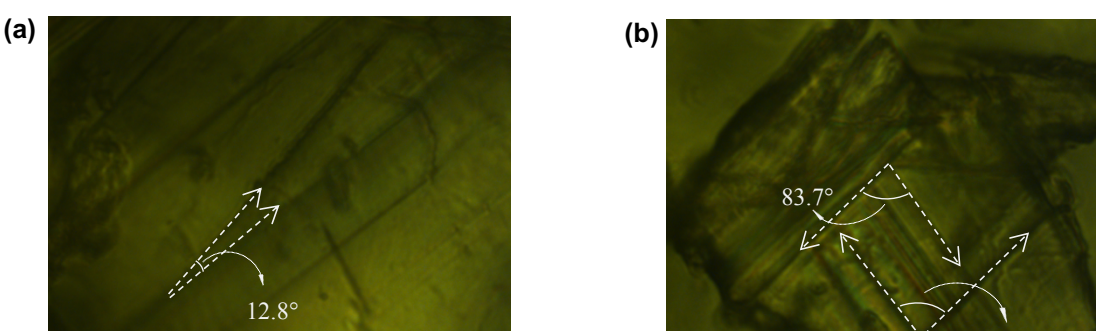

Figure 5. (a, b) Optical micrographs of twin crystals measured by using a polarized light microscope with 100x (NA=1.25) objective in the ambient condition.

In conclusion, we have comprehensively studied the complex phase transition in a hybrid organic-inorganic perovskite, $[CH_3NH_3][Mn(N_3)_3]$ (**1**), *via* a combined approach of experiments and lattice dynamics calculations. This unusual first-order phase transition involves concerted cooperation of molecular displacement, octahedral tilting and atomic vibration, making it distinct to those in oxide counterparts and other HOIPs. In particular, the difference in vibrations of all atomic sites between the HT and LT phases induces significant energetic changes, hence becoming the main driving force of the transition. Moreover, the large entropic effect, arising solely from vibrational entropy, across the transition is rare in molecular systems since entropy changes normally originate from configurational alterations related to different molecular ordering states. Taking the advantage of abundant chemical diversity of HOIPs, this study unveils a little corner of their giant phase transition landscape and highlights the fundamentally different new features of these transitions from an atomic level. Furthermore, considering the fact that many important properties of perovskites (e. g. ferroelectricity and multiferroicity) are a consequence of phase transitions, the cooperative contributions of all A-, B- and X-sites for driving phase transitions in HOIPs can give rise to many novel functionalities that conventional perovskites are unable to endow. Finally, viewing from a broad perspective, we believe this interplay between thermodynamic driving mechanisms – balancing entropy, electrostatics and inter-molecular bonding – can stimulate

and guide the discovery of new ferroic HOIPs and other hybrid materials.

Methods

Methods, including statements of data availability and any associated accession codes and references, are available in the online version of this paper.

References

1. Saparov, B. & Mitzi, D. B. Organic–inorganic perovskites: structural versatility for functional materials design. *Chem. Rev.* **116**, 4558–4596 (2016).
2. Li, W. et al. Chemically diverse and multifunctional hybrid organic–inorganic perovskites. *Nat. Rev. Mater.* 16099 (2017).
3. Xu, W.-J., Du, Z.-Y. & Zhang, W.-X. et al. Structural phase transitions in perovskite compounds based on diatomic or multiatomic bridges[J]. *CrystEngComm* **18**, 7915 (2016).
4. Whitfield, P. S. et al. Structures, Phase Transitions and Tricritical Behavior of the Hybrid Perovskite Methyl Ammonium Lead Iodide. *Sci. Rep.* **6**, 35685 (2016).
5. Boström, H. L. B., Hill, J. A. & Goodwin, A. L. Columnar shifts as symmetry-breaking degrees of freedom in molecular perovskites[J]. *Phys. Chem. Chem. Phys.* **18**(46): 31881-31894 (2016).
6. Gómez-Aguirre, L. C. et al. Coexistence of three ferroic orders in the multiferroic compound $[(CH_3)_4N][Mn(N_3)_3]$ with perovskite-like structure. *Chem. Eur. J.* **22**, 1–9 (2016).
7. Jain, P., Dalal, N. S., Toby, B. H., Kroto, H. W. & Cheetham, A. K. Order–disorder antiferroelectric phase transition in a hybrid inorganic–organic framework with the perovskite architecture. *J. Am. Chem. Soc.* **130**, 10450–10451 (2008).
8. Fu, D. et al. A multiferroic perdeutero metal–organic framework. *Angew. Chem. Int. Ed.* **50**, 11947–11951 (2011).
9. Zhang, W. & Xiong, R. Ferroelectric metal–organic frameworks. *Chem. Rev.* **112**, 1163–1195 (2012).
10. Butler, K. T., Svane, K, Kieslich, G. et al. Microscopic origin of entropy-driven polymorphism in hybrid organic-inorganic perovskite materials[J]. *Phys. Rev. B* **94**(18): 180103 (2016).
11. Zhao, X. et al. Cation-dependent magnetic ordering and room-temperature bistability in azido-bridged perovskite-type compounds. *J. Am. Chem. Soc.* **135**, 16006–16009 (2013).
12. Howard, C. J. & Stokes, H. T. Group-theoretical analysis of octahedral tilting in perovskites. *Acta Crystallogr. B* **54**, 782–789 (1998).
13. Stokes, H. T., Hatch, D. M., Campbell, B. J. 2007. ISOTROPY. <http://www.stokes.byu.edu/isotropy.html>.
14. Migilori, A., Sarraro, J. L. Resonant ultrasound spectroscopy: applications to physics, material measurements and non-destructive evaluation. New York: Wiley; 1997.
15. Carpenter, M. A. Static and dynamic strain coupling behaviour of ferroic and multiferroic perovskites from resonant ultrasound spectroscopy. *J. Phys.: Condens. Matter.* **27**, 263201 (2015).
16. Li, W. et al. Ferroelasticity in a metal–organic framework perovskite; towards a new class of multiferroics. *Acta Materialia* **61**, 4928–4938 (2013).

17. Thomson, R. I., Jain, P., Cheetham, A. K. & Carpenter, M. A. Elastic relaxation behavior, magnetoelastic coupling, and order-disorder processes in multiferroic metal-organic frameworks. *Phys. Rev. B* **86**, 214304 (2012).
18. Kieslich, G. et al. Role of entropic effects in controlling the polymorphism in formate ABX_3 metal-organic frameworks. *Chem. Commun.* **51**, 15538-15541 (2015).
19. Butler, K.T., Walsh, A., Cheetham, A. K. & Kieslich, G. Organised chaos: entropy in hybrid inorganic–organic systems and other materials. *Chem. Sci.* **7**, 6316-6324 (2016).
20. Stoumpos, C. C., Malliakas, C. D. & Kanatzidis, M. G. Semiconducting tin and lead iodide perovskites with organic cations: phase transitions, high mobilities, and near-infrared photoluminescent properties. *Inorg. Chem.* **52**, 9019–9038 (2013).
21. Jain, P. et al. Multiferroic behavior associated with an order−disorder hydrogen bonding transition in metal−organic frameworks (MOFs) with the perovskite ABX_3 architecture. *J. Am. Chem. Soc.* **131**, 13625-13627 (2009).
22. Harrison, R. J., Redfern, S. A. T., Salje, E. K. H. Dynamical excitation and anelastic relaxation of ferroelastic domain walls in $LaAlO_3$[J]. *Phys. Rev. B* **69**(14): 144101 (2004).

Acknowledgements

We acknowledge financial support from NSFC (Grant Nos. 21571072, 11374114 and 10974062).